arXiv:1111.1420v1 [nlin.CD] 6 Nov 2011

Generic Structures in Parameter Space and Ratchet Transport

A. Celestino[1], C. Manchein[1,2], H.A. Albuquerque[1] and M.W. Beims[2]
[1] *Departamento de Física, Universidade do Estado de Santa Catarina, 89219-710 Joinville, SC, Brazil and*
[2] *Departamento de Física, Universidade Federal do Paraná, 81531-980 Curitiba, PR, Brazil*

(Dated: November 8, 2011)

This work reports the existence of Isoperiodic Stable Ratchet Transport Structures in the parameter spaces dissipation *versus* spatial asymmetry and *versus* phase of a ratchet model. Such structures were found [Phys. Rev. Lett. **106** 234101 (2011)] in the parameter space dissipation *versus* amplitude of the ratchet potential and they appear to have generic shapes and to align themselves along preferred directions in the parameter space. Since the ratchet current is usually larger inside these structures, this allows us to make general statements about the relevant parameters *combination* to obtain an efficient ratchet current. Results of the present work give further evidences of the suggested generic properties of the isoperiodic stable structures in the context of ratchet transport.

PACS numbers: 05.45.Ac,05.45.Pq
Keywords: Shrimps, ratchet currents, transport.

Ratchet models are prominent candidates to describe the transport phenomenum in nature in the absence of external bias. The ratchet effect is a rectification of an external net-zero force to obtain a directional motion of particles in spatially periodic media. Spatiotemporal symmetries must be broken [1–3] in the system in order to obtain the *Ratchet Current* ($\mathcal{RC}$). In recent years the literature related to the ratchet transport has increased enormously as a consequence of promising applications. The $\mathcal{RC}$ was observed theoretically and experimentally in a variety of areas: in Brownian [4–9] and molecular motors [10], cold atoms in optical ratchets [11–17], spin ratchets [18], flow density [19], organic electronic ratchets [20], Levy ratchets [21, 22], Leidenfrost motion on ratchets [23, 24], granular gas [25], micro and nanofluids transport [26–30], Fermi acceleration [31], coupled to finite baths [32–35], magnetic films [36], energy transport [37–39], classical and quantum ratchets in general [40–44], among others.

Physical quantities like viscosity, particles mass, dissipation γ, noise intensity, amplitude of external forces K_t, ratchet potential amplitude K etc., are usually, depending on the system, the parameters which control the dynamics and the $\mathcal{RC}$. Normally these quantities are deeply interconnected so that small parameters variations may totally alter the dynamics and the efficiency of the $\mathcal{RC}$. Thus it is very desirable, if possible, to make general statements about the parameters *combination* which generate large $\mathcal{RC}$s. An imperative development in this direction suggested [45] that *Isoperiodic Stable Structures* (ISSs) in the parameter space present generic features which should be valid for almost all inertia ratchet models, independent of their application in nature. The ISSs are Lyapunov stable islands with dynamics globally structurally stable. One of the generic features found is the "pattern", or the "shape" of the ISSs. An example of such generic shape is the shrimp-shaped ISS [see Figs. 4(b) and 6(b)], which has already appeared in the parameter space of generic dynamical systems and applications [46–56], and observed recently in experiments with electronic circuits [57, 58]. A second apparently generic feature is that ISSs appear along preferred direction in parameter space, serving as a guide to follow the $\mathcal{RC}$ which is usually larger inside the ISSs. In this perspective, the main goal of the present work is to show that the ISSs found [45] in the parameter space (K, γ) and (K_t, χ) (this for the Langevin equation), present the same generic behavior in another parameter spaces, namely (a, γ) and (ϕ, γ), where a is the ratchet asymmetry and ϕ is the phase of the ratchet potential. This is of relevance not only to show the generic properties of the ISSs but for experimental realizations, where for specific experiments it is easier to vary different parameters. We show a direct connection between $\mathcal{RC}$s with a family of ISSs and chaotic domains in the above mentioned parameter spaces.

The paper is organized as follows: Section I presents the model which will be used and in Sec. II analytical results are derived for the stability boundaries in parameter space for fixed points. Section III shows the largest Lyapunov exponents (LEs) in the parameter space (K, γ), results which were not presented in [45], proving that the ISSs are stable. Sections IV and V present the $\mathcal{RC}$, LEs and periods of the orbits in the parameter spaces (a, γ) and (ϕ, γ), respectively. Section VI summarizes the main results and gives some perspectives for the experimental observation of ISSs.

I. THE MODEL

In order to show generic properties of the $\mathcal{RC}$ in the parameter space, we use a map M which presents all essential features regarding unbiased current [59]

$$M : \begin{cases} p_{n+1} = \gamma p_n + K[\sin(x_n) + a\sin(2x_n + \phi)], \\ x_{n+1} = x_n + p_{n+1}, \end{cases} \quad (1)$$

where p_n is the momentum variable conjugated to x_n, $n = 1, 2, \ldots, N$ represents the discrete time and K is the nonlinearity parameter. The dissipation parameter

γ reaches the overdamping limit for $\gamma = 0$ and the conservative limit for $\gamma = 1$. The ratchet effect appears due to the spatial asymmetry, which occurs with $a \neq 0$ and $\phi \neq m\pi$ ($m = 1, 2, \ldots$), in addition to the time reversal asymmetry for $\gamma \neq 1$. The $\mathcal{RC}$ of the above model was analyzed in the dissipation range $0 \leq \gamma < 1$, for fixed $K = 6.5$ [59] and in the parameter space $0 \leq \gamma < 1$ and $0 \leq K \leq 14$ [45]. It was shown that close to the limit $\gamma = 1$ the $\mathcal{RC}$ arises due to the mixture of chaotic motion with tiny island (accelerator modes) from the conservative case, while for smaller values of γ, chaotic and stable periodic motion (ISSs) generate the current.

The $\mathcal{RC}$ is obtained numerically from

$$\mathcal{RC} = \frac{1}{M}\sum_{j=1}^{M}\left[\frac{1}{N}\sum_{n=1}^{N} p_n^{(j)}\right], \tag{2}$$

where M is the number of initial conditions. At next we determine the $\mathcal{RC}$ for different parameter spaces always using a grid of 600×600 points, 10^5 initial conditions with $< p_0 >=< x_0 >= 0$ inside the unit cell $(-2\pi, 2\pi)$ and $N = 10^4$ iterations.

II. ANALYTICAL BOUNDARIES FOR FIXED POINTS ($\phi = \pi/2$)

Analytical boundaries for the $\mathcal{RC}$ in the parameter space can be determined for fixed points. They are obtained from the analytical expression for the eigenvalues of the Jacobian of the map (1) after one iteration. Using $\phi = \pi/2$ the fixed points from (1) can be calculated from

$$\begin{aligned} & p^{(1)} - 2\pi L = 0, \\ & 2\pi L(\gamma - 1) + K\left[\sin(x^{(1)}) + a\cos(2x^{(1)})\right] = 0, \end{aligned} \tag{3}$$

where L is an integer or rational number. The orbital solutions are

$$x_j^{(q=1)} = \arctan(\alpha^{(-)}, \pm\beta^{(+)}), \quad (j = 1, 2)$$

$$x_s^{(q=1)} = \arctan(\alpha^{(+)}, \pm\beta^{(-)}), \quad (s = 3, 4)$$

where

$$\alpha^{(\mp)} = K \mp \sqrt{f}, \qquad f = K\left[8Ka^2 + K + 16aL\pi(\gamma - 1)\right],$$

$$\beta^{(\pm)} = \sqrt{8aL\pi(1-\gamma) + 4Ka^2 - K \pm \sqrt{f}}.$$

The orbital points $x_{j,s}$ are plotted in Fig. 1 as a function of K, for $a = 0.5, \phi = \pi/2, \gamma = 0.2$ and $L = 1$. Dashed and dot-dashed lines are respectively the unstable points x_1, x_4, while thin and thick continuous lines are respectively the stable points x_2, x_3. We see that at $K = 6.0$ all four fixed points are born while for $K = 10$ the stable and unstable points x_3, x_4 collide and vanish (observe that is mod 2π). The points x_1, x_2 remain for higher values of K. Increasing the values of L, points x_1, x_2, x_3, x_4 move to higher values of K, but the bifurcation structure remains the same.

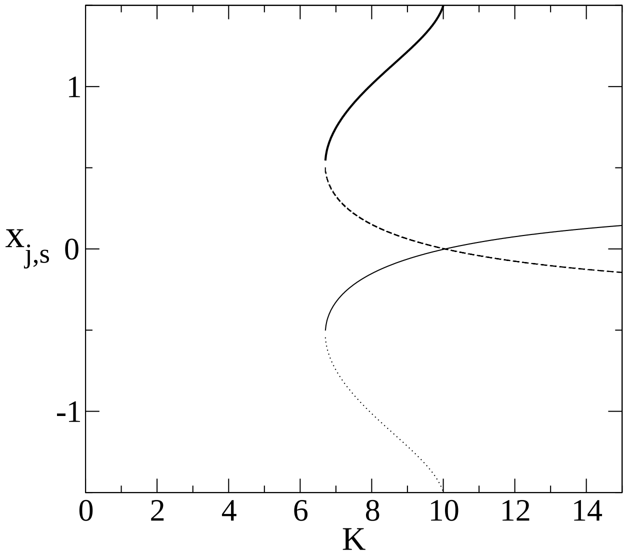

Figure 1. Fixed points x_1 (dashed line), x_2 (thin continuous), x_3 (thick continuous), x_4 (dot) as a function of K for $a = 0.5, \phi = \pi/2, \gamma = 0.2$ and $L = 1$.

Substituting the solutions (4) in the Jacobian of the map (1) after one iteration, we obtain analytical expressions for the eigenvalues $\lambda(K, \gamma, L)$. These expressions are very large and are not written explicitly here.

A. Born of period-1, any L.

When the eigenvalues satisfy the relation $\lambda(K, \gamma, L) = +1$, fixed points (or period-1 orbits) are born in the phase space. From this relation it is possible to determine $\gamma(K, L)$, which defines the boundaries in the parameter space for which fixed points are born. The solutions for the equation $\lambda(K, \gamma, L) - 1 = 0$, for all fixed points $x_j^{(q=1)}$, are

$$\gamma_{\pm 1}^{(1)}(L \neq 0, K, a) = 1 + \frac{K}{2\pi L}(a \pm 1), \tag{4}$$

$$\gamma_2^{(1)}(L \neq 0, K, a) = 1 - \frac{K}{2\pi L}\left(a + \frac{1}{8a}\right). \tag{5}$$

For $L = 0$ we found just the solution $a = 1$, independent of γ and K.

B. Bifurcation-1 → 2, $L = 0$.

When the eigenvalues satisfy $\lambda(K\gamma, L) = -1$, a double period bifurcation $1 \rightarrow 2$ occurs in phase space. For

$L \neq 0$ we were not able to find analytical expressions for $\gamma(K, L)$. However, for $L = 0$ the analytical solution are given by

$$\gamma^{(1\to2)}(K,a) = -1 + \frac{K}{8a}\left(\xi\sqrt{\xi^2 - 2\xi - 3}\right), \qquad (6)$$

where $\xi = \sqrt{8a^2 + 1}$.

The curves $\gamma^{(1)}_{\pm1}, \gamma^{(1)}_{2}$ and $\gamma^{(1\to2)}$ define exactly sharp period-1 boundaries in the parameter space. They generalize the curves shown in [45] to any K and a values and will be presented later together with numerical results. We were not able to find analytical solutions for the boundaries as a function of arbitrary ϕ.

III. PARAMETER SPACE $(\mathbf{K}, \gamma)$

The purpose of this section is to show that the ISSs presented in [45] are *stable*. To do this we present the LEs in parameter space. For comparison, we start showing in Fig. 2(a) the $\mathcal{RC}$ plotted in colors for the parameter space (K, γ) with $\phi = \pi/2$ and $a = 1/2$. This is the parameter space analyzed in [45] but for a larger K interval. While black colors represent close to zero currents, red to yellow colors are related to increasing negative currents. Green to white colors are related to increasing positive currents (see color bar). An unusual complex structure of colors is evident. Three distinct behaviors can be identified: (*i*) a large "cloudy" background, identified as A in Fig. 2, mixed with black, red and green colors, showing a mixture of zero, small negative and positive currents, respectively; (*ii*) ISSs B_L (cusp-like), C_L and D_L (shrimp-like) embedded in the cloudy background regions; (*iii*) strong positive and negative currents (region E), with not well defined borders which occur close to the conservative limit $\gamma = 1$. All ISSs are related to periodic [45] and stable motion. The stable behavior can be seen in Fig. 2(b), which is the parameter space for the LE. Black to white are related to negative LEs and blue, green, yellow to red related to increasing LEs. All ISSs from Fig. 2(a), where the $\mathcal{RC}$ becomes usually larger inside, can be identified with the negative LEs regions from Fig. 2(b). Thus the ISSs maintain their "shape" *independently* if we measure the $\mathcal{RC}$ or the LEs in the parameter space. The same is observed for the periods of the orbits, shown in Fig. 2 from [45]. All analytical boundaries for the B_L ISSs are obtained directly from $\gamma^{(1)}_{-1}(L \neq 0, K, a)$ and $\gamma^{(1)}_{2}(L \neq 0, K, a)$ given in Sec. II. Four of them are plotted as red straight lines in Fig. 2(b).

In the cloudy background region A from Fig. 2(a), smaller $\mathcal{RC}$s are observed and can be directly identified with the regions of positive LEs from Fig. 2(b). These $\mathcal{RC}$s are the consequence of the asymmetry of the chaotic attractor [17]. Thus we clearly see that the cloudy chaotic background is not efficient to generate the $\mathcal{RC}$ as the ISSs are, and that the magnitude of the positive LEs do not change the values of the corresponding $\mathcal{RC}$s. For region E the $\mathcal{RC}$ in Fig. 2(a) is shown to be enhanced, but the structures does not have well defined borders. When compared to Fig. 2(b) we observe that the region E is chaotic. The origin of the large $\mathcal{RC}$ is due to accelerator modes which exist in the conservative limit $\gamma = 1$ and are responsible for the asymmetry of chaotic attractors.

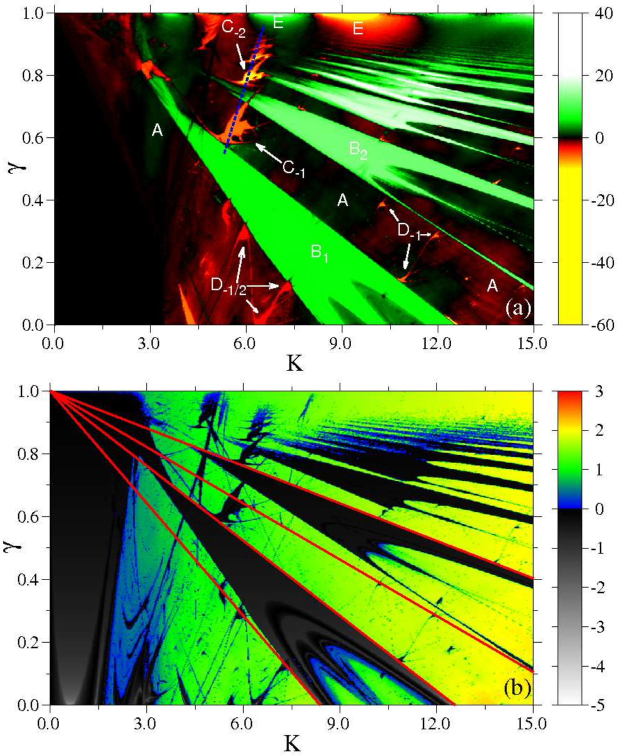

Figure 2. (Color online) (a) The $\mathcal{RC}$ and (b) largest Lyapunov exponent plotted in the parameter space (K, γ).

IV. PARAMETER SPACE (a, γ)

The $\mathcal{RC}$ in the parameter space (a, γ) is shown in Figure 3(a) (see colorbar). Three main regions, as observed in Fig. 2(a), are identified: the large cloudy background region A, mixed with black, red and green colors, showing a mixture of zero, small negative and positive currents, respectively; ISSs with well defined borders and embedded in the cloudy background region; and finally region E with strong positive and negative currents with not well defined borders which occur close to the conservative limit $\gamma = 1$. Figure 3(b) shows the corresponding parameter space (a, γ) for the LEs, where black to white are related to negative LEs and blue, green, yellow to red related to increasing LEs. Fig. 3(c) shows the corresponding parameter space for the period q of the orbits. Periods q are identified by green: $q = 1$, blue: $q = 2$, cyan: $q = 3$, yellow: $q = 4$, pink: $q = 6$, red $q \geq 8$ and black for no period. In Fig. 3(c) only one initial condition is used $(x_0 = 0.5, p_0 = 0.3)$, $N = 10^6$ iterations and a grid of 600×600 points. Comparing Figs. 3(a),(b) and (c) a direct connection between the $\mathcal{RC}$ with the chaotic and the regular periodic behavior can be made. All ISSs appear with negative (black to white) LEs and periodic motion while the cloudy background with small values of the $\mathcal{RC}$s and region E, are related to the chaotic motion and no periodic motion.

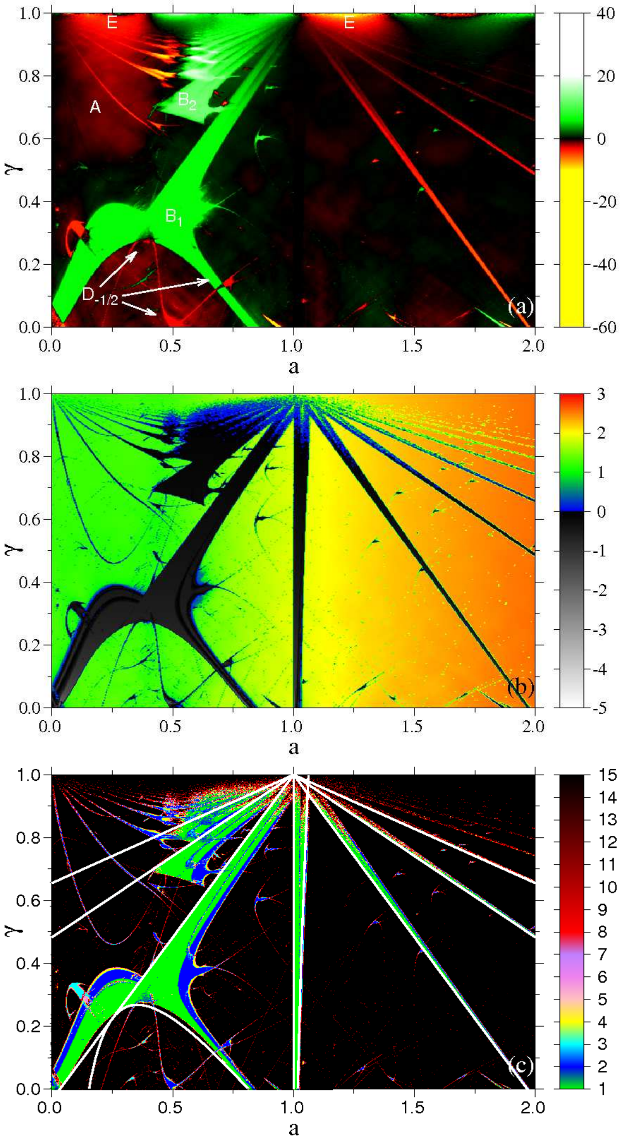

Figure 3. (Color online) (a) The $\mathcal{RC}$, (b) largest Lyapunov exponent and (c) period q of the orbits (see text) plotted in the parameter space (a, γ) for $K = 6.5$ and $\phi = \pi/2$.

Larger green ISSs are observed for $a < 1$, which apparently are responsible for the large positive $\mathcal{RC}$s. Thinner red ISSs exist for $a > 1$. Close to $a = 1$ we also observe to have a ISS with zero $\mathcal{RC}$. Inside all these ISSs a period doubling bifurcation cascade 1×2^n $(n = 1, 2, \ldots)$ occurs, always starting from the left, as can be observed in Fig. 3(c). These left boundaries, where fixed points are born, were obtained analytically in Sec. II and some of them are plotted as white line in Fig. 3(c). When using $L = 1, 2, 3, \ldots$ in $\gamma_{-1}^{(1)}$ from Eq. (5), we obtain *all* left boundaries for $a < 1$, while using $L = -1, -2, -3, \ldots$ in $\gamma_{-1}^{(1)}$ we obtain *all* left boundaries for $a > 1$. For $L = 0$ we also found the left boundary located at $a = 1$, which has current exactly zero inside. For this case with $L = 0$ we were able to find the boundary of bifurcation $1 \to 2$, given by Eq. (6) and is plotted as a solid white line in Fig. 3(c). The $\mathcal{RC}$ is exactly zero inside the ISSs with $L = 0$ because points of the periodic attractor are located exactly symmetrically around zero, independent of the period. There occurs a *whole* symmetric period doubling bifurcation inside this ISS, for any dissipation value. Symmetric period doubling bifurcation means that orbital points are symmetrically located around $p = 0$, thus the $\mathcal{RC}$ is zero. ISSs with analytical boundaries clearly have the B_L cusp shape, where the inner part of the cusp is stretched out. Going to the conservative limit $\gamma \to 1$ where $L \to \pm\infty$, it is easy to show analytically, using results from Sec. II, that the approximation rate $(B_{L+1} - B_L)/(B_L - B_{L-1})$ approaches 1.

The other ISSs, namely C_L and D_L (shrimp-like), also appear in the parameter space (a, γ). The shrimp-shaped ISSs are immersed in the cloudy background region A. There are many of such structures as can be better seen in the LE parameter space from Fig. 3(b). As γ decreases these ISSs follow preferred directions. The C_L

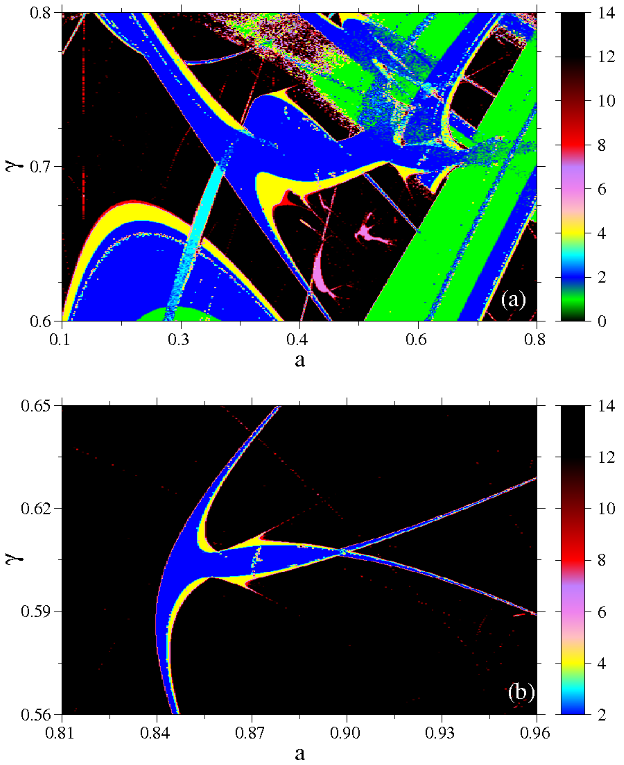

Figure 4. (Color online) Magnifications of Fig. 3(c) showing (a) C_L and (b) D_L (shrimp) ISSs.

ISSs are harder to be observed, but can be recognized in the magnification shown in Fig. 4(a). In this case we used $K = 5.6, \phi = \pi/2 - 0.3$, which is more appropriate to recognize the C_L structures. In fact, we found out that the C_L ISS is an overlap of the shrimp-like ISS and the inverted cusp [60]. As γ, K (and ϕ) change they may start to go apart (close) and separate (join). This is similar to what occurs for the shrimp-like structure, which is an overlap of the cusp with the inverted cusp, which are generated by cubic maps [61, 62]. On the other hand, Fig. 4(b) shows a magnification of the typical shrimp-shaped ISS.

Also in the parameter space (a, γ) we observe that the magnitude of the LE does not increase/decrease the $\mathcal{RC}$ in region A. Compare the LEs for $a < 1$ with those for $a > 1$, they are distinct but the corresponding $\mathcal{RC}$s are essentially equal. Close to the conservative limit $\gamma = 1$, we again observe a chaotic motion, as in the case of Fig. 2(a), with larger $\mathcal{RC}$s, which are generated due to the mixture of the chaotic motion with the transporting islands from the conservative limit.

V. PARAMETER SPACE (ϕ, γ)

Figure 5(a) shows the parameter space (ϕ, γ) for the $\mathcal{RC}$. First observation is that the $\mathcal{RC}$ is anti-symmetric under the transformation $\phi \to 2\pi - \phi$, and thus current reversals occur when $\phi \to 2\pi - \phi$. A nice unusual structure is observed. As for all other parameter spaces shown here, Fig. 5(a) displays three main regions: the large cloudy background region A, mixed with black, red and green colors, showing a mixture of zero, small negative and positive currents, respectively; the ISSs with well defined borders and embedded in the cloudy background region; and finally region E with strong positive and negative currents with not well defined borders which occur close to the conservative limit $\gamma = 1$. Figure 5(b) shows the parameter space (ϕ, γ) for the LE (see colorbar) while Fig. 5(c) displays the corresponding periods of the orbits. Comparing with Fig. 5(a) a direct connection of the $\mathcal{RC}$ with the regular periodic and chaotic behavior can be made. All ISSs appear with negative (black to white) LEs (Fig. 5(b)) and periodic motion in Fig.5(c), while the cloudy background with small values of the $\mathcal{RC}$s and region E are related to chaotic and non-periodic motion. The magnitude of the LE does not increase/decrease the $\mathcal{RC}$ in region A. Close to the conservative limit $\gamma = 1$ the large $\mathcal{RC}$s are again generated due to the mixture of the chaotic motion with the transporting islands from the conservative limit.

In this case it was not possible to determine analytically the boundaries of the cusp ISSs. However, combining Figs. 2,3 and 5 it is possible to recognize that the large red (green) ISSs from Fig. 5(a), which look very similar to "rips", belong to the cusps. The first (from below) and larger cusp appears deformed and connected to shrimps [see white box in Fig. 5(c)]. As $\gamma \to 1$ these ISSs approach to each other. The C_L and D_L (shrimp-like) ISSs also appear in the parameter space (ϕ, γ) as can be recognized in the magnifications shown in Fig. 6. For better visualization of the C_L ISS, the magnification from Fig. 6(a) was calculated along the line $K = (\gamma + 0.994925)/0.2845$. This line was obtained from Fig. 2 by making a fit (see blue dotted line) along the preferred direction of the ISSs in that parameter space. On the other hand, Fig. 6(b) shows a typical D_L shrimp ISS. Besides the above properties, the three plots show a remarkable combination of ISSs structures showing the rich and controlled dynamics which may be generated by tailoring the parameters.

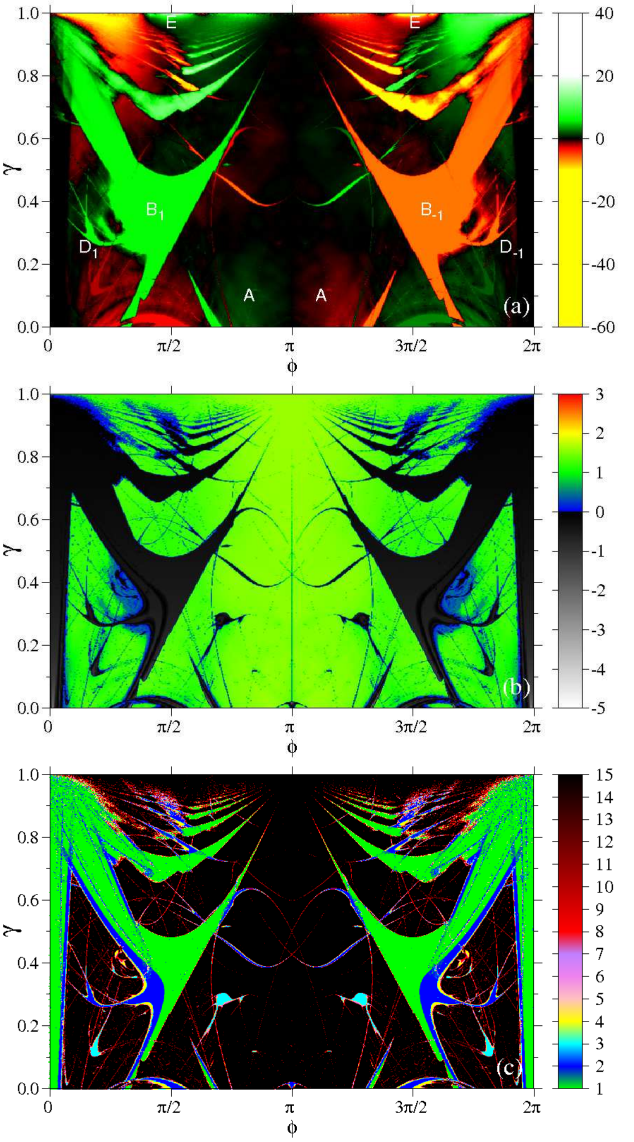

Figure 5. (Color online) (a) The $\mathcal{RC}$, (b) Lyapunov exponents and (c) period q of the orbits (see text) plotted in the parameter space (ϕ, γ) for $K = 6.5$ and $a = 0.5$.

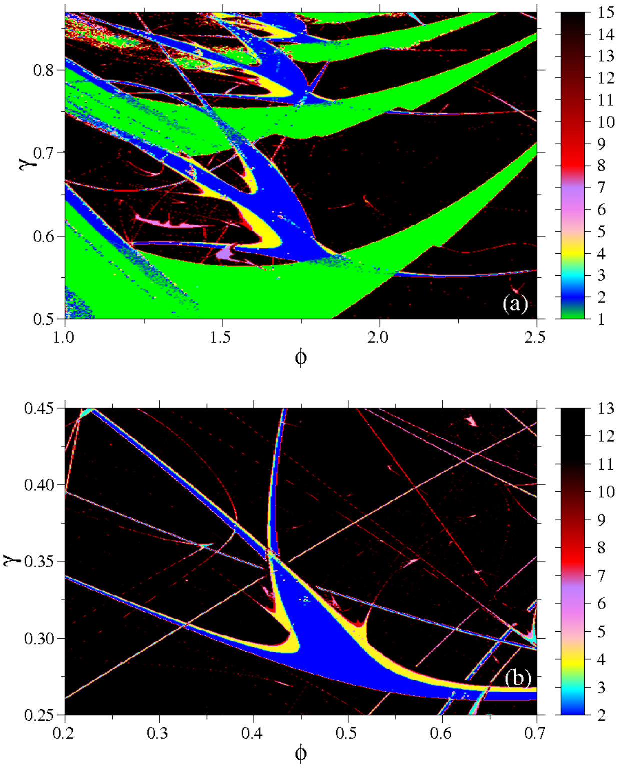

Figure 6. (Color online) Magnifications of Fig. 5(c) showing (a) C_L and (b) D_L (shrimp) ISSs.

VI. CONCLUSIONS

It was suggested recently [45] that ISSs, inside which the $\mathcal{RC}$ is usually larger, should present generic features in almost all parameter spaces of ratchet systems which display dissipation γ against a parameter related to the ratchet property. In that work two parameter spaces were analyzed: (K,γ) for the discrete model (1), where K is the amplitude of the ratchet potential and (K_t,χ) for the Langevin equation, where K_t is the amplitude of the external time dependent oscillating force with zero mean. In the present work we show that the ISSs appear also in the parameter spaces (a,γ) and (ϕ,γ), where a and ϕ give, respectively, the spatial asymmetry and phase of the ratchet potential (see Eq. 1). We show a direct connection between $\mathcal{RC}$s with a family of ISSs and chaotic domains in the above mentioned parameter spaces. In all cases studied we observe that the ISSs usually follow three important properties: (1) their *pattern* (shrimps, cusps, etc..) remains the same, independent of the parameter space studied, (2) their *appearance* along preferred directions in the parameter space, serving as a guide to search for larger $\mathcal{RC}$s and (3) for smaller dissipations the $\mathcal{RC}$ increases significantly inside the ISSs, even though they are not responsible for the larger $\mathcal{RC}$ observed, but the accelerator modes from the conservative limit. Besides that it was also observed that in chaotic regions the $\mathcal{RC}$s are smaller compared to the regions with ISSs. The magnitude of the positive LEs also do not affect the $\mathcal{RC}$. This complete connection between $\mathcal{RC}$s with a family of ISSs and chaotic domains in parameter spaces gives us general clues for the origin of directed transport and further evidences of the generic properties of the ISSs to generate such transport.

Besides the ratchet experiments with cold atoms [63] or with the net motion of the particles in a silicon membrane with asymmetric pores [64], suggested in [45] as candidates to observe the generic ISSs experimentally, we would like to mention here another recent experimental device for this purpose. It is the Leidenfrost motion of solids and droplets [23, 24] on a hot ratchet-like plate. We guess that determining the terminal velocity of the drops in the parameter space temperature of the plate against the radius of the drop, it should be possible to see reminiscences of the ISSs.

[1] L.Cavallasca, R.Artuso, and G.Casati, Phys.Rev.E **75**, 066213 (2007).
[2] L. Wang, G. Benenti, G. Casati, and B. Li, Phys. Rev. Lett. **99**, 244101 (2007).
[3] S.Flach, O.Yevtushenko, and Y.Zolotaryuk, Phys.Rev.Lett. **84**, 2358 (2000).
[4] J.M.Polson, B.Bylhouwer, M.J.Zuckermann, and J. andA.J.Horton W.M.Scott, Phys.Rev.E **82**, 051931 (2010).
[5] X.Z.Cheng, M.B.A.Jalil, and H.K.Lee, Phys.Rev.Lett. **99**, 070601 (2007).
[6] R.D.Astumian and P.Hänggi, Phys.Today **55**, 33 (2002).
[7] H. Linke, Appl. Phys. A **75**, 167 (2002).
[8] P.Reimann, Phys.Rep. **361**, 57 (2002).
[9] M. O. Magnasco, Phys. Rev. Lett. **71**, 1477 (1993).
[10] F.Jülicher, A.Ajdari, and J.Prost, Rev.Mod.Phys. **1997**, 1269 (1997).
[11] M.Rietmann, R.Carretero-Gonzalez, and R.Chacon, Phys.Rev.A **83**, 053617 (2011).
[12] H.Hagman, M.Zelan, C.M.Dion, and A.Kastberg, Phys.Rv.E **83**, 020101 (2011).
[13] M. abd H.Hagman, G.Labaigt, S.Jonsell, and C.M.Dion, Phys.Rev.E **83**, 020102(R) (2011).
[14] R. Gommers, V. Lebedev, M. Brown, and F. Renzoni, Phys. Rev. Lett. **1**, 040603 (2008).
[15] L.Morales-Molina and S.Flach, New Journal of Physics **10**, 013008 (2008).
[16] A.V.Gorbach, S.Denisov, and S.Flach, Optics Letters **31**, 1702 (2006).
[17] G.G.Carlo, G.Benenti, G.Casati, and D.L.Shepelyansky, Phys.Rev.Lett. **94**, 164101 (2005).
[18] M.V.Costache and S.O.Valenzuela, Science **330**, 1645 (2010).
[19] H.J.Chen, J.L.Huang, C.Y.Wang, and H.C.Tseng, Phys.Rev.E **82**, 052103 (2010).
[20] E.M.Roeling, W.C.Germs, B.Smalbrugge, E.J.Geluk,

J.Erik, T. Vries, R.A.J.Janssen, and M.Kemerink, Nature Materials **10**, 51 (2011).
[21] I.Pavlyukevich, B.Dybiec, and A.V.Chechkin, Europ.Phys.J **191**, 223 (2010).
[22] S.Denisov, S.Flach, A.A.Ovchinnikov, O.Yevtushenko, and Y.Zolotaryuk, Phys.Rev.E **66**, 041104 (2002).
[23] G.Lagubeau, M. L. Merrer, C. Clanet, and D. Quere, Nature Physics **7**, 395 (2011).
[24] H. Linke, B. J. Alemnán, L. D. Melling, M. J. F. M. J. Taormina, C. C. Dow-Hygelund, V. Narayanan, and R. P. T. e A. Stout, Phys. Rev. Lett. **96**, 154502 (2006).
[25] P.Eshuis, K. der Weele, D.Lohse, and D. der Meer, Phys.Rev.Lett. **104**, 248001 (2010).
[26] K.Mathwig, F.Muller, and U.Gosele, New Journal of Physics **13**, 033038 (2011).
[27] Q.Guo, S.M.McFaul, and H.S.Ma, Phys.Rev.E **83**, 051910 (2011).
[28] G.Lambert, D.Liao, R.H.Austin, and H.Robert, Phys.Rev.Lett. **104**, 168102 (2010).
[29] K.John, P.Hänggi, and U.Thiele, Soft Matter **4**, 1183 (2008).
[30] J. C. T. Eijkel and A. van den Berg, Microfluid Nanofluid **1**, 249 (2005).
[31] C.Manchein and M.W.Beims, Math. Prob. Eng. **2009**, 513023 (2009).
[32] C. Manchein, J. Rosa, and M. W. Beims, Physica D **238**, 1688 (2009).
[33] J. Rosa and M. W. Beims, Phys. Rev. E **78**, 031126 (2008).
[34] J. Rosa and M. W. Beims, Physica A **386**, 54 (2007).
[35] J. Rosa and M. W. Beims, Physica A **342**, 29 (2004).
[36] A. Perez-Junquera, V. Marconi, A. Kolton, L. Alvarez-Prado, Y. Souche, A. Alija, M. Velez, J. Anguita, J. Alameda, J. Martin, et al., Phys. Rev. Lett. **1**, 037203 (2008).
[37] A.V.Gorbach, S.Denisov, and S.Flach, Chaos **16**, 023125 (2006).
[38] G. A. Denisov S, Flach S, Europhys.Lett. **72**, 183 (2005).
[39] S.Flach, Y.Zolotaryuk, A.E.Miroshnichenko, and M.V.Fistul, Phys.Rev.Lett. **88**, 184101 (2002).
[40] G.G.Carlo, L.Ermann, F.Borondo, and R.M.Benito, Phys.Rev.E **83**, 011103 (2011).
[41] H. Schanz, M.-F. Otto, R. Ketzmerick, and T. Dittrich, Phys. Rev. Lett. **87**, 070601 (2001).
[42] J. Lehmann, S. Kohler, and P. H. P. and, Phys. Rev. Lett. **88**, 228305 (2002).
[43] S.Kohler, J.Lehmann, and P.Hänggi, Phys.Rep. **406**, 379 (2005).
[44] P. Reimann, M. Grifoni, and P. Hanggi, Phys. Rev. Lett. **79**, 10 (1997).
[45] A.Celestino, C. Manchein, H.A.Albuquerque, and M.W.Beims, Phys.Rev.Lett. **106**, 234101 (2011).
[46] J.A.C.Gallas, Phys.Rev.Lett. **70**, 2714 (1993).
[47] S.Hayes, C.Grebogi, and E.Ott, Phys.Rev.Lett. **70**, 3031 (1993).
[48] J. A. C. Gallas, Physica A **202**, 196 (1994).
[49] J. A. C. Gallas, Appl. Phys. B **60**, S203 (1995).
[50] M. S. Baptista and I. L. Caldas, Chaos, Solitons & Fractals **7**, 325 (1996).
[51] M. W. Beims and J. A. C. Gallas, Physica A **238**, 225 (1997).
[52] M. W. Beims, P. C. Rech, and J. A. C. Gallas, Physica A **294**, 272 (2001).
[53] C.Bonatto and J.A.C.Gallas, Phys.Rev.E **75**, R055204 (2007).
[54] C. Bonatto, J. A. C. Gallas, and Y. Ueda, Phys. Rev. E **77**, 026217 (2008).
[55] C.Stegemann, H.A.Albuquerque, and P.C.Rech, Chaos **20**, 023103 (2010).
[56] R.Vitolo, P.Glendinning, and J.A.C.Gallas, Phys.Rev.E **84**, 016216 (2011).
[57] R.Stoop, P.Benner, and Y.Uwate, Phys.Rev.Lett. **105**, 074102 (2010).
[58] E. Jr, R.M.Rubinger, H.A.Albuquerque, and A.G.Oliveira, Chaos **20**, 023110 (2010).
[59] L. Wang, G. Benenti, G. Casati, and B. Li, Phys.Rev.Lett. **99**, 244101 (2007).
[60] A.Endler and J.A.C.Gallas, C.R.Acad.Sci.Paris, Ser.I **342**, 681 (2006).
[61] E. N. Lorenz, Physica D **237**, 1689 (2008).
[62] F.Cabral, A.Lago, and J.A.C.Gallas, Journal of Modern Physics C: Physics and Computers **4**, 553 (1993).
[63] C.Mennerat-Robilliard, D.Lucas, S.Guibal, J.Tabosa, C.Jurczak, J.-Y.Courtois, and G.Grynberg, Phys.Rev.Lett. **82**, 851 (1999).
[64] S.Matthias and F.Müller, Nature **424**, 53 (2003).